Available online at www.sciencedirect.com
SCIENCE DIRECT®
Talanta 65 (2005) 246–254
Talanta
www.elsevier.com/locate/talanta

Methodology of multicriteria optimization in chemical analysis Some applications in stripping voltammetry

M. Cruz Ortiz*, Ana Herrero, Silvia Sanllorente, Celia Reguera

Department of Chemistry, Faculty of Sciences, University of Burgos, Plaza Misael Bañuelos s/n, 09001 Burgos, Spain

Received 15 March 2004; received in revised form 25 May 2004; accepted 22 June 2004
Available online 9 August 2004

Abstract

Multicriteria optimization, widely used in engineering, does not much used in the optimization of analytical signals. The aim of this paper is to show the usefulness of the desirability function to optimize instrumental responses obtained in instrumental analysis. The simultaneous optimization of a signal and of its variability is a generic question of interest to any chemical analyst. It is clear that the improvement of the two responses forms the basis of the validation of any analytical method, and affects all the figures of merit: accuracy (trueness and precision), capability of detection, robustness, sensitivity, etc. Furthermore, in the specific case of electroanalysis, an improvement in the signal may implicitly mean an increase of the signal in the blank, such that the "net signal" may not improve. This experimental approach (surface response methodology plus desirability) to multicriteria optimization has been applied to three cases of growing complexity. Thus, in the determination of Cu(II) by differential pulse anodic stripping voltammetry the simultaneous maximization of the peak current and minimization of its standard deviation is looked for. Whereas, in the determinations of Ni(II) and indomethacin by differential pulse adsorptive stripping voltammetry, the simultaneous maximization of the peak current and minimization of the blank signal is desired. In all the cases, the experimental conditions where the optima are found for each individual response are just opposite, so it is required to look for a certain compromise, that is achieved using the desirability function.

Keywords: Experimental design; Optimization; Desirability; Optimal path; Stripping voltammetry

1. Introduction

Nowadays electroanalytical techniques have a wide field of application in chemical analysis. At the beginning the most classic techniques were principally used for the determination of inorganic species. However, the evolution of electroanalytical instrumentation has led to the development of selective procedures which are highly sensitive and very reproducible to also determine a large number of organic species. Thus, stripping voltammetric techniques have a step of preconcentration of the analyte or analytes to be determined that leads to sensitivities in the order of fractions of parts per billion [1]. But when using these electroanalytical techniques several experimental factors that influence and interact have to be optimized.

Different methods for solving single objective optimization problems have been applied in electroanalysis [2]. However, single objective decision-making methods reflect an earlier and simpler era because nowadays the performance of chemical analysis has become more complex. More so analysts find it imperative to evaluate alternative analytical procedures according to multiple criteria, the response selection being a critical stage in the optimization process since the main aim of optimization is to find the experimental conditions which give the best response.

Frequently the aim of optimization in stripping voltammetry is to reach lower detection limits, hence the need to use multicriteria optimization functions since in general it is not usually enough to optimize the magnitude of the signal (frequently a peak current). In many cases it is necessary to

* Corresponding author. Fax: +34 947 258831.
E-mail address: mcortiz@ubu.es (M.C. Ortiz).

0039-9140/$ – see front matter © 2004 Elsevier B.V. All rights reserved.
doi:10.1016/j.talanta.2004.06.031

take into account at the same time other aspects of the analysis such as reducing the variability of the signal, minimising the contribution of the experimental blank, maximising the signal/noise ratio, etc.

To do this, experimental design methodology is very useful, more specifically response surface analysis [3,4]. However, it is usual that the experimental conditions that optimize the signal are not similar to those that optimize other possible aspects to be considered, so it is necessary to solve the conflict established between the different objectives. To solve this conflict one can use desirability functions [5,6]. In this work, the Derringer desirability function [7] is used, which implies: (i) clearly defining what results are acceptable for each individual response (magnitude of the signal, its variance, blank signal, etc.); (ii) defining what values would not be at all acceptable; and (iii) fitting a continuous function between (i) and (ii) conditions.

The overall desirability function D is defined as the weighted geometric average of the individual desirability functions (d_i)

$$D = \sqrt[n]{d_1^{p_1} \times d_2^{p_2} \times \cdots \times d_n^{p_n}} \quad (1)$$

p_i being the weight corresponding to each of them. Through the individual functions, the analyst introduces the specifications that each response must fulfil in the measuring procedure. However, despite the obvious advantages of this methodology in chemical analysis, there are still few applications found in the bibliography [8–11].

This multicriteria methodology has been used in this work to optimize determination of Cu(II) by differential pulse anodic stripping voltammetry (DPASV) and the determinations of nickel and indomethacin by differential pulse adsorptive stripping voltammetry (DPAdSV). In the case of copper, both the magnitude of the peak current and its variance were simultaneously optimized (the first maximised and the second minimised), whereas in the other two cases, the simultaneously optimized responses were the peak current (maximised) and the blank signal (minimised). In all the cases, acceptable overall desirability values have been obtained.

2. Experimental

2.1. Reagents and equipment

Analytical and suprapur grade chemicals were used with no further purification. All the solutions were prepared with deionised water obtained using a Barnstead NANO Pure II system. Nitrogen (99.99%) was used to remove dissolved oxygen.

Copper solutions were prepared by dissolving analytical grade copper powder in a minimum volume of HNO_3 and diluting with water to give the desired concentration (1×10^{-6} mol l^{-1}). The complexing agent EDTA was used as supporting electrolyte.

Stock solutions of nickel were prepared by dissolving the adequate amount of analytical grade nickel powder in the minimum volume of HNO_3 and filling up with deionised water. This solution was diluted with water to give the desired concentration (9×10^{-11} mol l^{-1}). The solution of complexing agent, DMG in this case, was obtained by dissolving the appropriate amount of dymethylglyoxime in 96% methanol. Ammonia-ammonium chloride buffer 0.01 mol l^{-1} solution was used as supporting electrolyte.

Analytical grade indomethacin was kindly provided by Merck Sharp and Dome. The corresponding stock solutions were prepared in analytically pure grade acetonitrile that were subsequently diluted with deionised water to the desired concentration (5×10^{-8} mol l^{-1}). Britton-Robinson solutions were used as buffers.

Voltammetric measurements were carried out using a Methrom 646 VA Processor with a 647 VA Electrode Stand in conjunction with a multimode electrode (MME) operating in the HMDE mode. The three-electrode system was completed by means of a platinum auxiliary electrode and an Ag/AgCl/KCl (3 mol l^{-1}) reference electrode.

Data analysis was achieved with NemrodW [12] and Progress [13].

2.2. Experimental procedure

Each sample was placed in a voltammetric cell and purged with nitrogen for ten minutes. Once the solution had been deoxygenated the stirrer was connected and a deposition potential, E_{dep}, was applied to the working electrode for time, t_{dep}. The stirring rate was 1290 rpm the mercury drop size was 0.40 mm^2 in all the analyses.

Some of the instrumental parameters were previously optimized through preliminary experiments. In the case of the determination of copper [14], at the end of the accumulation period, the stirrer was switched off and, after 20 s had elapsed, an anodic potential scan was initiated from E_{dep} (initial potential) to 0.1 V (final potential), with scan rate 10 mV s^{-1}, pulse amplitude 50 mV, and pulse repetition time 0.6 s. In the case of nickel [15], the equilibrium time was 10 s, afterwards being applied a cathodic potential scan from E_{dep} to –1.1 V, with scan rate 8 mV s^{-1}, pulse amplitude 60 mV and pulse repetition time 0.3 s. And for indomethacin [16], the equilibrium time was 10 s, the applied cathodic potential being from −1.0 to −1.6 V, with scan rate 10 mV s^{-1}, pulse amplitude 50 mV and pulse repetition time 0.6 s.

3. Results and discussion

3.1. Determination of Cu(II) by differential pulse anodic stripping voltammetry

When using the DPASV technique, the response obtained for a determined analyte, the peak current, is usually influenced by a large number of variables of different nature that

Table 1
Experimental matrix and experimental responses of the experimental design for the determination of copper

Run	Factors			Responses	
	C_{EDTA} (mol l^{-1})	E_{dep} (V)	t_{dep} (s)	Peak current (nA)	Standard deviation (nA)
1	8.10×10^{-6}	−0.350	30	40.65	0.483
2	8.16×10^{-4}	−0.350	30	88.81	2.190
3	8.10×10^{-6}	−1.000	30	62.14	0.160
4	8.16×10^{-4}	−1.000	30	125.23	1.660
5	8.10×10^{-6}	−0.350	180	220.87	6.350
6	8.16×10^{-4}	−0.350	180	259.30	1.450
7	8.10×10^{-6}	−1.000	180	238.13	6.490
8	8.16×10^{-4}	−1.000	180	374.30	10.760
9	4.12×10^{-4}	−0.675	105	136.60	4.010

have to be taken into account: pH, concentration of supporting electrolyte, deposition time and potential, rest period, pulse amplitude, pulse repetition time, scan rate, etc.

Prior analysis [14] of copper in the presence of EDTA as supporting electrolyte showed that the variables t_{dep}, E_{dep} and concentration of EDTA, C_{EDTA}, could have a significant effect on the analysed response, the peak height. However, a very relevant characteristic of the signal, its variance, was then obviated. Thus, an optimization study when maximising the peak current and minimising its variance are desired is carried out here. This is useful in chemical analysis in order to increase the sensitivity and reduce the variability of the analytical procedure, i.e. to reach better detection limits and more precise determinations.

3.1.1. Single objective models

In a first step of the analysis, the peak current and its variance were analysed independently, building a mathematical model for each objective in order to study if the optimum points reached individually for each factor coincide in both cases. Thus, a 2^3 factorial design with a central point was carried out following the experimental matrix shown in Table 1. Each experiment was carried out in random order and three replicates (that is, the reapplication of the preconcentration and stripping stages to the same solution) were obtained. In this way, the mathematical model

$$y = \beta_0 + \beta_1 x_1 + \beta_2 x_2 + \beta_3 x_3 \quad (2)$$

was built taking as response the peak current (mean of the three replicates), whereas a second model was built taking as response the standard deviation estimated with the three replicates.

Least squares regression for standard deviation shows a R^2 = 0.63 and the model is not significant (P-level = 0.14 with the F test). An analysis of the residuals done by least median of squares regression (LMS) [13] shows that the values of the runs 6 and 8 have standardized residuals of −18.9 and 8.8, respectively, well above the threshold value of 2.5. In addition, the values of the index of resistance to diagnose are also above 2.5 (6.9 and 3.6, respectively). The model without these two outlier data, showed in Table 2, has a R^2= 0.981. It can be seen that the inflation factor of the variance of the coefficients (VIF) is still close to one, i.e. the properties of the design have not worsened by eliminating both points.

Table 2
Estimates and statistics of the coefficients from the fitted response surfaces for peak current and standard deviation for the determination of copper

Response	Coefficient		F. inflation	S.D.	P-level
Peak current	b_0	161.82		5.52	<0.001
	b_1 (C_{EDTA})	24.53	1.07	5.92	0.014
	b_2 (E_{dep})	12.57	1.07	5.92	0.101
	b_3 (t_{dep})	85.77	1.07	5.92	<0.001
Standard deviation	b_0	4.14		0.09	<0.001
	b_1 (C_{EDTA})	0.79	1.29	0.10	0.005
	b_2 (E_{dep})	−0.11	1.00	0.09	0.269
	b_3 (t_{dep})	3.03	1.29	0.10	<0.001

In the case of the peak current, run 8 has a standardized residual of 5.66 and a value of the index of resistance to diagnose 4.24. Since both are above 2.5, this point has been removed and the model recalculated with the rest of the data. The coefficient of determination, R^2, of the model goes from 0.947 to 0.981 and the model is very significant (P-level < 0.001).

The significance of the coefficients for both models is shown in Table 2, where it can be concluded that in both cases the only significant factors are C_{EDTA} and t_{dep}. However, when analysing the response surfaces corresponding to the two fitted models, Fig. 1, where the factor E_{dep} is maintained fixed at a value of −0.68 V (it has been found not significant), it can be seen that the experimental conditions that maximise the peak current and minimise its standard deviation are just opposite. This makes the fact that the individual analysis of the responses does not lead to common experimental conditions clear, so a multicriteria methodology that looks for certain compromise experimental conditions that fulfil the expectations of the analyst is required.

3.1.2. Multicriteria optimization: desirability function

This multicriteria methodology is based on constructing a desirability function for each individual response. Each individual desirability function is a continuous function chosen from among a family of linear or exponential functions and varies from zero (undesirable response) to 100 (optimal response). Based on these individual desirability functions, the overall desirability function is estimated as the weighted geometric average of the individual desirability functions, as has been pointed out in Section 1. NemrodW [12] uses a simulated annealing algorithm in the optimization process to find the optimum of the overall desirability function, since this is not derivable.

In this case, linear desirability functions were chosen for both responses. In the case of peak current, values below 180 nA have been considered not acceptable (zero desirability), while values above 200 nA are optimal; the desirability function varying linearly between these two values. However,

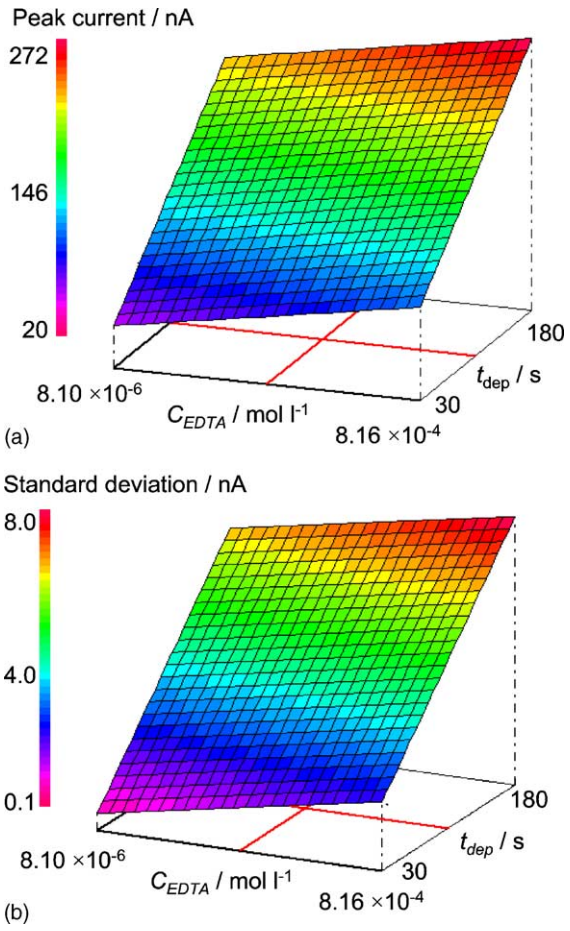

Fig. 1. Estimated response surfaces fitted individually for the peak current (a) and the standard deviation (b) in the determination of copper. The third factor, E_{dep}, is maintained in both cases at a potential of −0.68 V.

in the case of the standard deviation of the peak current, values below 3.6 nA are acceptable because they are equivalent to a maximum of 2% of the signal (it must be remembered that they are scans in the same cell and hence their dispersion must be small). For the same reason, it must be considered that standard deviations above 5 nA are not acceptable (zero desirability). As for the peak current, the function varies linearly between these two values. In addition, equal weights were given for the two responses since both are considered equally important in the overall desirability function, i.e. $p_1 = p_2 = 1$ in Eq. (1).

The maximum of the overall desirability function is found for $C_{EDTA} = 8.13 \times 10^{-4}$ mol l^{-1}, $t_{dep} = 111$ s and $E_{dep} = -0.477$ V, the peak current being at this point 200 nA and the corresponding standard deviation 3.6 nA. Under these experimental conditions the constraints imposed on the individual desirability functions are totally fulfilled and an overall desirability of 100% is reached. Fig. 2 shows the contour plot of the global desirability function in the space of the factors C_{EDTA} and t_{dep}. Although this representation is only partial since the factor E_{dep} remains constant, it shows that the optimum found is at the edge of the experimental domain for the

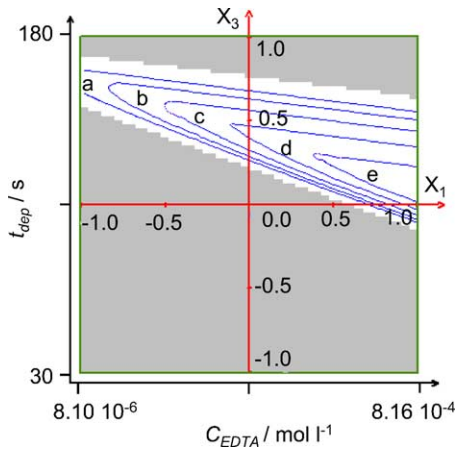

Fig. 2. Contour plot of the overall desirability function in the space of the factors C_{EDTA} and t_{dep}. Grey zone corresponds to zero desirability, and contour lines (a), (b), (c), (d) and (e) to 50, 60, 70, 80 and 90% of the overall desirability function. The E_{dep} is fixed at −0.48 V.

factor C_{EDTA}. In addition, this figure shows that it is possible to reach a desirability above 90% with concentrations of EDTA above 4.2×10^{-4} mol l^{-1} and t_{dep} varying to 125 s. Also, it is observed that one can reach a high desirability (above 70%) for a wide range of EDTA concentrations but for each of them the range of the t_{dep} is very specific and restricted. That is, the global desirability is very sensitive to small changes in the analysed factors, principally to changes in the t_{dep}.

One final comment, in the data in Table 1 one can see that run 6 fulfils the conditions required of the peak current and standard deviation. This experiment lies outside the linear trend shows by the rest, both for the peak current and the standard deviation. The global desirability function shows the possibility of a wide margin experimental in terms of C_{EDTA} and its corresponding t_{dep} associated according to the analysis of Fig. 2.

3.2. Determination of Ni(II) by differential pulse adsorptive stripping voltammetry

A second example of application of this multi-response methodology has been the optimization of the determination of nickel by DPAdSV, analysis based on the already known adsorption of the complex Ni(II)–DMG on the mercury electrode. In a previous experiment [15], several instrumental parameters were optimized to offer the greatest measurement reproducibility. In this work, since the metal is being determined at trace level, the optimization procedure is direct to simultaneously maximise the peak current of the analyte of interest, nickel peak, and to minimise the current of the blank at the nickel peak potential, blank current.

3.2.1. Single objective models

Firstly, as in the previous work, the peak current and the blank current were considered as responses independently to

Table 3
Experimental matrix and experimental responses of the experimental design for the determination of nickel

Run	Factors			Responses	
	C_{DMG} (mol l^{-1})	t_{dep} (s)	E_{dep} (V)	Peak current (nA)	Blank current (nA)
1	2.50×10^{-5}	30	−0.10	1.809	0.000
2	5.00×10^{-4}	30	−0.10	2.742	2.629
3	2.50×10^{-5}	300	−0.10	5.572	4.584
4	5.00×10^{-4}	300	−0.10	11.840	9.250
5	2.50×10^{-5}	30	−0.80	1.791	0.000
6	5.00×10^{-4}	30	−0.80	2.785	2.264
7	2.50×10^{-5}	300	−0.80	9.772	4.963
8	5.00×10^{-4}	300	−0.80	15.020	11.620
9	2.62×10^{-4}	165	−0.45	7.887	5.209
10	2.62×10^{-4}	165	−0.45	8.734	6.111
11	2.62×10^{-4}	165	−0.45	9.262	6.873

study the optima reached individually. In this case, a 2^3 factorial design was performed, each experiment being carried out in random order following the experimental matrix shown in Table 3. The mathematical model used in this case was

$$y = \beta_0 + \beta_1 x_1 + \beta_2 x_2 + \beta_3 x_3 + \beta_{12} x_1 x_2 + \beta_{13} x_1 x_3 + \beta_{23} x_2 x_3 \quad (3)$$

Similarly to the previous analysis, two independent models were built taking as response the peak current and the blank current, with the aim of maximising the first and minimising the second.

For the peak current, the model is significant (P-level 0.022) and does not show lack of fit (P-level 0.083). The value of R^2 is 0.940. The same occurs for the model estimated for the blank current, which is significant (P-level 0.024) and does not show lack of fit (P-level 0.174), R^2 being 0.938. There are neither outliers nor influential data for either of the two models.

The estimates of the coefficients of these two models and the corresponding statistics are shown in Table 4. It can be deduced from it that both t_{dep} and C_{DMG} influence the blank current significantly, but only the first of these factors has a significant influence on the peak current of nickel. In both models, neither the third factor, E_{dep}, nor the interactions are significant. On the other hand, analogously to what occurred in the previous example, when the response surfaces of the significant factors of the two fitted models are compared, Fig. 3, the experimental conditions that maximise one of the responses (the peak current) and minimise the other (the blank current) are opposite. So, the use of an optimization methodology to objectively find a compromise zone is also required in this case.

3.2.2. Multicriteria optimization: desirability function

In this second example, contrary to the other cases, individual curved desirability functions were chosen as shown in Fig. 4. For the peak current, values below 8 nA are considered not acceptable and those above 12 nA are considered optimal for the peak current, while values above 8 nA are not acceptable and those below 5 nA are considered optimal for the blank current. In both cases, the desirability functions vary between the indicated two values according to Fig. 4. Also, equal weights were given for the two responses.

The maximum of the overall desirability function (close to 93%) is reached for C_{DMG} = 2.50×10^{-5} mol l^{-1}, t_{dep} = 300 s and E_{dep} = −0.80 V, the peak current being under this experimental conditions 10.16 nA and the blank current

Table 4
Estimates and statistics of the coefficients from the fitted response surfaces for peak current and blank current for the determination of nickel

Response	Coefficient		F. inflation	S.D.	P-level
Peak current	b_0	7.0185		0.5170	<0.001
	b_1 (C_{DMG})	1.6804	1.00	0.6062	0.051
	b_2 (t_{dep})	4.1346	1.00	0.6062	0.003
	b_3 (E_{dep})	0.9256	1.00	0.6062	0.201
	b_{12}	1.1986	1.00	0.6062	0.118
	b_{13}	−0.1199	1.00	0.6062	0.846
	b_{23}	0.9194	1.00	0.6062	0.203
Blank current	b_0	4.8639		0.4271	<0.001
	b_1 (C_{DMG})	2.0270	1.00	0.5008	0.017
	b_2 (t_{dep})	3.1905	1.00	0.5008	0.042
	b_3 (E_{dep})	0.2980	1.00	0.5008	0.587
	b_{12}	0.8037	1.00	0.5008	0.183
	b_{13}	0.2032	1.00	0.5008	0.704
	b_{23}	0.3892	1.00	0.5008	0.484

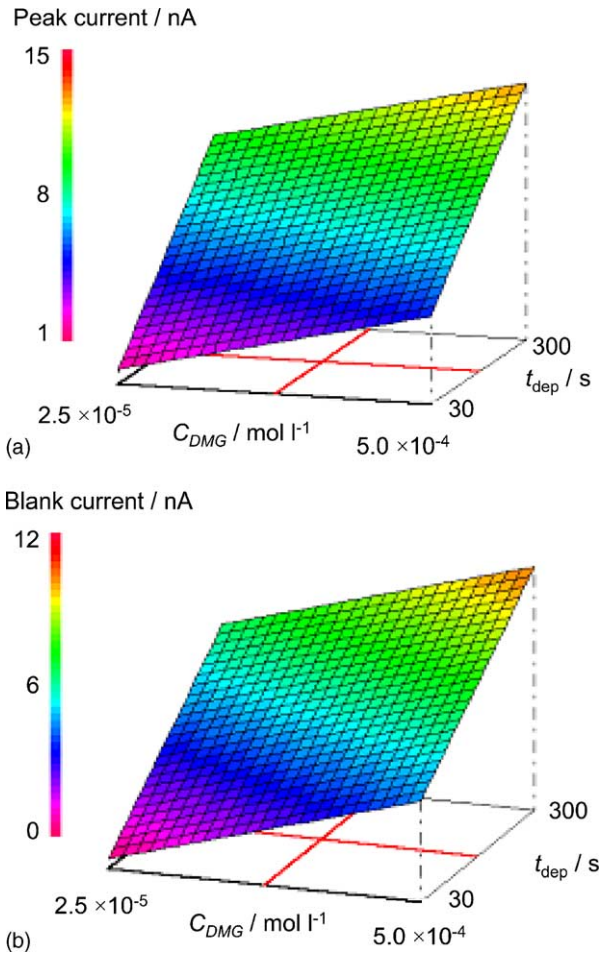

Fig. 3. Estimated response surfaces fitted individually for the peak current (a) and the blank current (b) in the determination of nickel. The third factor, E_{dep}, is maintained in both cases at a potential of −0.45 V.

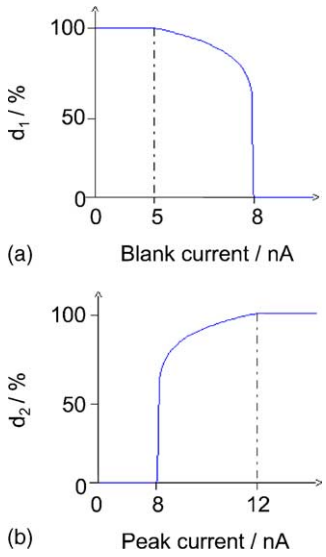

Fig. 4. Individual desirability functions for the blank current (a) and the peak current (b) in the determination of nickel.

6.32 nA. The corresponding contour plot for C_{DMG} and t_{dep} is shown in Fig. 5, where the compromise zone for these two factors can be seen when E_{dep} is fixed at −0.80 V.

The region in which 90% desirability is surpassed covers a wide interval for C_{DMG}, from 2.50×10^{-5} to 2.85×10^{-4} mol l^{-1}. However, for the first value we can use a t_{dep} between 232 and 300 s, while for the second only a t_{dep} of 219 s is valid, that is, it can notably reduce analysis time.

3.3. Determination of indomethacin by differential pulse adsorptive stripping voltammetry

The last example that has been studied in this work is the determination of an anti-inflammatory drug, indomethacin, by DPAdSV based on the adsorption of the molecule at the mercury electrode in aqueous media. Previous studies [16] showed that for acidic solutions the reduction on the electrode is essentially a two electron process that provides a voltammetric peak, but pH can have an effect both on the position of the peak as on the magnitude of the signal; the percentage of buffer in the electrochemical cell ($\%_{buffer}$) and the deposition time (t_{dep}) also being relevant factors that influence the voltammetric response.

The aim of this analysis is to optimize this determination taking into account two different responses, as in the previous example, on the one hand the peak current, and on the other the blank current. One is intended to maximize the first and to minimize the second, optimising the aforementioned factors: pH, $\%_{buffer}$ and t_{dep}. Thus, firstly the individual models for each response have been studied and next the multicriteria methodology has been applied, in a similar way to that carried out in the two previous examples.

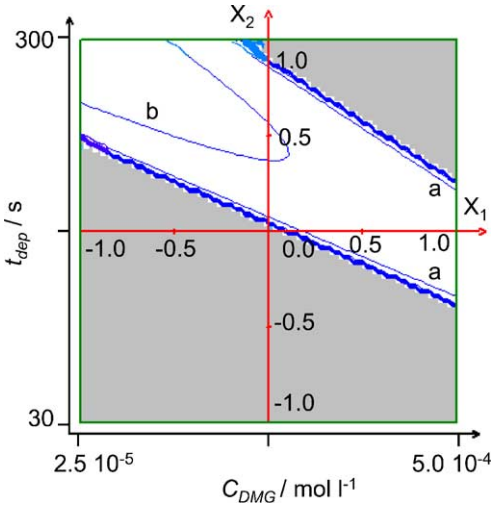

Fig. 5. Contour plot of the overall desirability function in the space of the factors C_{DMG} and t_{dep}. Grey zone corresponds to zero desirability, and contour lines (a) and (b) to 80 and 90% of the overall desirability function. The E_{dep} is fixed at −0.8 V.

Table 5
Experimental matrix and experimental responses of the experimental design for the determination of indomethacin

Run	Factors			Responses	
	pH	$\%_{buffer}$	t_{dep} (s)	Peak current (nA)	Blank current (nA)
1	6.0	45.0	200	13.76	10.00
2	6.0	45.0	90	12.74	9.26
3	6.0	25.0	200	14.43	6.95
4	6.0	25.0	90	10.10	5.32
5	4.0	45.0	200	65.79	8.74
6	4.0	45.0	90	35.92	8.58
7	4.0	25.0	200	69.35	19.08
8	4.0	25.0	90	42.19	9.34
9	6.7	35.0	145	11.25	5.08
10	3.3	35.0	145	48.62	6.66
11	5.0	51.8	145	48.09	9.03
12	5.0	18.2	145	47.72	5.78
13	5.0	35.0	237	20.77	24.95
14	5.0	35.0	52	11.00	11.25
15	5.0	35.0	145	52.19	7.05
16	5.0	35.0	145	41.82	5.45
17	5.0	35.0	145	42.19	6.12

Table 6
Estimates and statistics of the coefficients from the fitted response surfaces for peak current and blank current for the determination of indomethacin

Response	Coefficient		F. inflation	S.D.	*P*-level
Peak current	b_0	45.23		4.661	<0.001
	b_1 (pH)	−16.48	1.00	2.189	<0.001
	b_2 ($\%_{buffer}$)	−0.53	1.00	2.189	0.81
	b_3 (t_{dep})	5.77	1.00	2.189	0.033
	b_{11}	−4.88	1.16	2.409	0.081
	b_{22}	1.47	1.16	2.409	0.560
	b_{33}	−9.85	1.16	2.409	0.048
	b_{12}	1.47	1.00	2.860	0.625
	b_{13}	−6.46	1.00	2.860	0.057
	b_{23}	−0.07	1.00	2.860	0.978
Blank current	b_0	6.27		1.518	0.045
	b_1 (pH)	−1.23	1.00	0.713	0.125
	b_2 ($\%_{buffer}$)	0.10	1.00	0.713	0.887
	b_3 (t_{dep})	2.59	1.00	0.713	0.008
	b_{11}	−0.35	1.16	0.785	0.668
	b_{22}	0.19	1.16	0.785	0.810
	b_{33}	3.97	1.16	0.785	0.002
	b_{12}	2.26	1.00	0.931	0.004
	b_{13}	−0.94	1.00	0.931	0.348
	b_{23}	−1.31	1.00	0.931	0.201

3.3.1. Single objective models

In this case, a central composite design, that shown in Table 5, was carried out in random order. The mathematical model fitted was a complete second-order model

$$y = \beta_0 + \beta_1 x_1 + \beta_2 x_2 + \beta_3 x_3 + \beta_{12} x_1 x_2 + \beta_{13} x_1 x_3 + \beta_{23} x_2 x_3 + \beta_{11} x_1^2 + \beta_{22} x_2^2 + \beta_{33} x_3^2 \quad (4)$$

that, similarly to the previous examples, was fitted in a first stage of the analysis independently for the peak current and the blank current.

The significance of the coefficients corresponding to the two models is shown in Table 6. It can be seen that in the model built for the peak current, pH, t_{dep} and ${t_{dep}}^2$ are significant, whereas in the model built for the blank current, t_{dep} and ${t_{dep}}^2$ are significant as well as the interaction pH-$\%_{buffer}$. In both cases, the analysis of the variance carried out shows that the models are significant and do not have lack of fit at a significance level of 5%, the R^2 being equal to 92.90 and 88.88%, respectively.

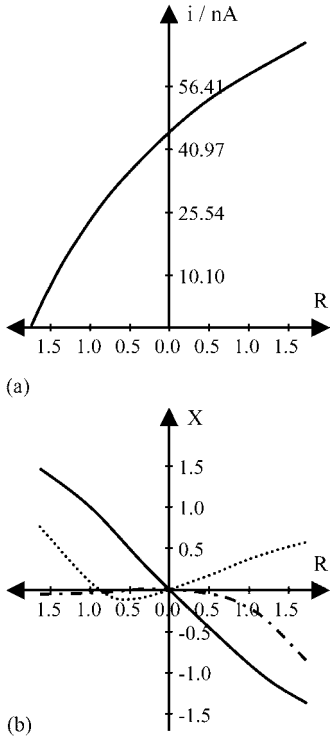

Fig. 6. (a) Optimum path of the response surface fitted to the peak current where ordinates represent the optimum response reached on the built spheres for radius *R* indicated in abscissas; (b) coordinates of the points of plot (a) for each factor in codified variables: (—) pH; (- · -) $\%_{buffer}$; (···) t_{dep}. The right part of both plots refers to the maximisation of the response; the left part of the plots refers to the minimisation of the response.

For the blank current model, the three factors are significant either through the linear or through the quadratic terms, so it is necessary to determine the optimum path of the response surface in a different way to the previous one. In this case, the optimum path of the response surface is determined by tracing spherical surfaces, centred on the central point of the experimental domain and with growing radius, and calculating on each of these the maximum and the minimum of the response surface [4,17].

Thus, the optimum paths of the response surface are shown in Figs. 6 and 7 for both individual models. It is clear that in the optimum path shown in Fig. 6, the maximum peak current, 67.25 nA, is reached at the boundary of the experimental domain, at distance 1.7 (right). The coordinates for this maximum, Fig. 6b, transformed into real variables correspond to pH = 3.66, $\%_{buffer}$ = 25% and t_{dep} = 172 s. To reach the maximum, the first two factors must have lower values while the deposition time must tend toward higher values.

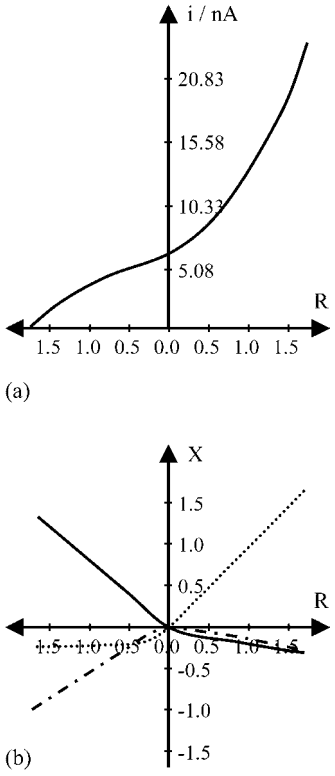

Fig. 7. (a) Optimum path of the response surface fitted to the blank current where ordinates represent the optimum response reached on the built spheres for radius R indicated in abscissas; (b) coordinates of the points of plot (a) for each factor in codified variables: (—) pH; (- · -) $\%_{buffer}$; (···) t_{dep}. The right part of both plots refers to the maximisation of the response; the left part of the plots refers to the minimisation of the response.

However, Fig. 7 shows that the minimum blank current, 0.49 nA, is reached at distance 1.7 (left) that corresponds to pH = 6.41, $\%_{buffer}$ = 25% and t_{dep} = 139 s. Fig. 7b shows that at distances close to the minimum the blank current is more sensitive to variations in pH and percentage of the buffer than to changes in the deposition time. In any case, it is clear that neither in this example are common experimental conditions found for the desired optimization of the two responses: the percentage of buffer is the same in both cases, the deposition time is not too different taking into account its experimental range, but the pH values found in each case are really different. Thus, comparing the lines corresponding to pH in Figs. 6b and 7b, it is clear that higher values of pH lead to minimising the blank current but also the peak current, whereas lower values of pH have less influence on the blank current and maximise the peak current.

3.3.2. Multicriteria optimization: desirability function

In this third example linear desirability functions were chosen. For the peak current, values below 40 nA have been considered not acceptable, while values above 60 nA are optimal; and for the blank current, values above 12 nA are not acceptable, while values below 8 nA are optimal. In both cases, the desirability functions vary linearly between the two values indicated. Also weights were given equal for the peak current and the blank current.

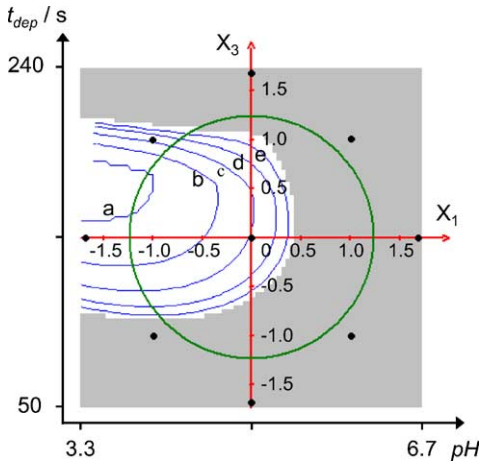

Fig. 8. Contour plot of the overall desirability function in the space of the factors pH and t_{dep}. Grey zone corresponds to zero desirability, and contour lines (a), (b), (c), (d) and (e) to 100, 80, 60, 40 and 20% of the overall desirability function. The $\%_{buffer}$ is fixed at 47.1%.

The maximum of the overall desirability function is reached for pH = 4.01, $\%_{buffer}$ = 47.1% and t_{dep} = 181 s, the peak current being under these experimental conditions 60.22 nA and the blank current 7.84 nA, i.e. this solution fulfils all the restrictions imposed to build the individual desirability functions, reaching overall and individual desirabilities of 100%. Fig. 8 shows a graphic study of the variability of the overall desirability function in the space of pH and t_{dep}. Although the factor $\%_{buffer}$ remains constant in this plot, it can be seen that in the region around the optimum, only acceptable results are obtained, the optimum being more sensitive to changes in t_{dep} than to changes in pH.

It could seem strange that the value of the factor $\%_{buffer}$ corresponding to the optimum is so far from the unique value reached with the two individual models (25% in both cases). However this points out that the overall desirability function really searches for a global solution for all the responses considered that is independent of the possible individual solutions.

3.4. Final consideration

When looking for the working conditions for an analytical procedure, it is normal to consider various criteria to be optimized. It is also normal that the experimental conditions which lead to an optimum for one of them are not the same as for another. In this case the desirability function is always useful. Whether the compromise solution is satisfactory or not depends on the specific analytical problem and on the requirements for the analysis. The advantage of the method proposed is that it introduces the analytical requirements just as they are posed. That is, what is not acceptable and what is. This specifically implies choosing “experimental zones”

in which the response is “not valid” “progressively valid” or “completely acceptable”.

This “a priori” decision is also the main limitation to the procedure because other possibilities which may be of interest once the experimentation is complete are not explored. In other words, the alternative is to explore the set of non dominated optimum solutions (Pareto front) and afterwards decide which of them to use. This option is being studied by our research group. However, it has the drawback of not giving acceptable regions, but rather optimum points. The advantage of having regions with a pre-set desirability is clear. One only has to look at Figs. 2, 5 and 8 and their analysis in the text.

Another alternative is to reduce the responses to just one by combining them “ad hoc”. This may conceal undesired situations. For example, in problems such as case (i), the variation coefficient could be chosen as the response to be optimised. The drawback is that if one multiplies by the same factor the signal and its standard deviation, one gets the same coefficient of variation but the variability may be unacceptable (the procedure may have bad repeatability).

Acknowledgements

The authors thank the Ministerio de Ciencia y Tecnología (Project BQU2003-07073) and Junta de Castilla y León (Project BU 06/04).

References

[1] J. Wang, Stripping Analysis. Principles, Instrumentation and Applications, VCH, Deerfield Beach, FL, 1985.
[2] S.D. Brown, R.S. Bear, Crit. Rev. Anal. Chem. 24 (1993) 99.
[3] S.N. Deming, S.L. Morgan, Experimental Design: A Chemometric Approach, Elsevier, New York, 1987.
[4] R.H. Myers, D.C. Montgomery, Response Surface Methodology, Wiley, New York, 1995.
[5] T.B. Barker, Quality by Experimental Design, 2nd ed, Marcel-Dekker, New York, 1994.
[6] S. Ghosh (Ed.), Statistical Design and Analysis of Industrial Experiments, Marcel-Dekker, New York, 1990 (Chapter 9).
[7] G. Derringer, R. Suich, J. Qual. Tech. 12 (1980) 214.
[8] A.M. Carro, I. Neira, R. Rodil, R.A. Lorenzo, Chromatographia 56 (2002) 733.
[9] M.E. Rueda, L.A. Sarabia, A. Herrero, M.C. Ortiz, Anal. Chim. Acta 479 (2003) 173.
[10] E. Rueda, M.C. Ortiz, L.A. Sarabia, A. Herrero, Anal. Chim. Acta 498 (2003) 119.
[11] C.H. Kuo, S.W. Sun, Anal. Chim. Acta 482 (2003) 47.
[12] D. Mathieu, J. Nony, R. Phan-Tan-Luu, NemrodW, ver. 2000, LPRAI, Marseille, 2000.
[13] P.J. Rousseew, A.M. Leroy, Robust Regresión and Outlier Detection, Wiley, New York, 1987.
[14] A. Herrero, M.C. Ortiz, M.J. Arcos, J. López-Palacios, Analyst 119 (1994) 1585.
[15] S. Sanllorente, M.C. Ortiz, M.J. Arcos, J. López-Palacios, Electroanalysis 8 (1996) 285.
[16] C. Reguera, M.J. Arcos, M.C. Ortiz, Talanta 46 (1998) 1493.
[17] G.A. Lewis, D. Mathieu, R. Phan-Tan-Luu, Pharmaceutical Experimental Design, Marcel-Dekker, New York, 1999.